Tetrahedron Letters 53 (2012) 6383–6387

Contents lists available at SciVerse ScienceDirect

Tetrahedron Letters

journal homepage: www.elsevier.com/locate/tetlet

2,6-Diarylethynylanthracenes: synthesis, morphology, and electro-optical properties

Bhanupriya Khanna [a], Sean R. Parkin [b], Kevin D. Revell [a,*]

[a] Department of Chemistry, 1201 Jones Hall, Murray State University, Murray, KY 42071, USA
[b] Department of Chemistry, University of Kentucky, Lexington, KY 40506, USA

ARTICLE INFO

Article history:
Received 13 August 2012
Revised 7 September 2012
Accepted 10 September 2012
Available online 17 September 2012

Keywords:
Cross-coupling
Alkynes
Chromophores
Semiconductors

ABSTRACT

A series of 2,6-diarylethynyl-9,10-dialkoxyanthracenes have been synthesized, characterized, and evaluated for their morphological and electro-optical properties. Compounds with 2′-naphthyl and 2′-anthracyl peripheral substituents were found to have poor solubility, and were not explored in detail. However, compounds bearing 9′-anthracyl peripheral substituents exhibited better solubility, and a series of these compounds containing straight-chain and branched substituents were prepared and analyzed. These compounds were found to undergo two oxidations at +0.57 V and +0.76 V relative to a Fc/Fc^+ reference. The compounds exhibited absorption with a λ_{onset} of 510 nm. Based on this, the average solution-phase HOMO–LUMO energies of these compounds were estimated to be −5.37 eV and −2.94 eV, respectively. The compounds exhibited fluorescent behavior, with an emission maximum at 505 nm. Hexoxy and Isobutoxy substituents were optimal for large crystal formation, and crystallographic studies on these two compounds show a herringbone-type arrangement with 1-dimensional pi-stacking.

© 2012 Elsevier Ltd. All rights reserved.

Recently, numerous studies have explored the semiconducting properties of acenes and arylacetylenes for application in devices including photovoltaic cells, light-emitting diodes, and thin-film transistors.[1–7] These compounds have been shown to meet criteria essential to design functionality, including appropriate HOMO–LUMO energy gaps and crystal packing motifs which enhance charge mobility through the solid. Promising semiconducting properties were recently reported for thin films of 9,10-bis(arylethynylanthracenes)[8] and 2,6,9,10-tetra(arylethynylanthracenes).[9–11] In our own efforts in this area, we wished to examine the physical properties of anthracenes having an extended pi system linked in the 2 and 6 positions, and solubilizing alkoxy substituents in the 9 and 10 positions. In particular, we wished to understand what effects the different substitution patterns might have on solubility, crystal packing, and HOMO–LUMO energy levels. This Letter describes the synthesis and preliminary physical characterization of these compounds.

The 2,6-dibromo-9,10-dihexoxyanthracyl core (**1a**) was initially prepared by reduction of 2,6-dibromoanthraquinone, followed by addition of hexyl triflate, following previously described methods. [11–12],[†] Sonogashira coupling[‡] of compound **1a** with two equivalents of 2-ethynylnaphthalene or 2-ethynylanthracene proceeded smoothly and in modest yields to give products **2** and **3** as bright yellow solids (Scheme 1).

Unfortunately, these compounds were only slightly soluble in organic solvents such as chloroform, dichloroethane, toluene, etc. Although most impurities could be removed by digestion and filtration of the target product, suitable conditions for more rigorous purification by recrystallization were not found.

The poor solubility of **2** and **3** led to the postulate that compound set **4**, in which the anthracyl side chains are linked at the 9′- rather than the 2′-position, might improve both solubility and solid-phase pi-overlap as compared to **2** and **3**. To explore this possibility, compound **4a** was prepared through a similar Sonogashira coupling (Scheme 2). It was found that **4a** exhibited better solubility than either **2** or **3**, and was easily crystallized from a mixture of

* Corresponding author. Tel.: +1 270 809 6540; fax: +1 270 809 6474.
E-mail address: kevin.revell@murraystate.edu (K.D. Revell).

† This conversion was also examined using the less expensive hexyl bromide as alkylating agent using DMF:H_2O in a variety of ratios and at different temperatures. It was found that conversion using the bromide (5 equiv) could be accomplished optimally in 80:20 DMF:water, using 8 equiv K_2CO_3 as base at rt for 16 h. However, reproducibility was very poor, and yields decreased sharply on scale-up.

‡ General procedure for Sonogashira couplings: a mixture of halide (1 equiv), $PdCl_2(PPh_3)_2$ (0.02 equiv), and copper(I) iodide (0.06 equiv) was taken up in degassed, anhydrous THF (2 mL/mmol halide). This solution was sealed and deoxygenated by evacuation/backfill using an inert gas (6x). Triethylamine (5 equiv) was added by syringe, and the deoxygenation procedure was repeated. The acetylene (2.4 equiv) was then added, and the resulting solution was heated to 80 °C under an inert atmosphere for 16 h. The mixture was cooled, diluted with hexanes and/or dichloromethane, and extracted with 1 M aq. HCl, followed by water and brine. The organic layer was filtered to remove any remaining solids, then was dried over anhydrous Na_2SO_4 and concentrated. Purification was accomplished by recrystallization from 1,2-DCE and *n*-hexane. Spectroscopic data for these compounds are given in the Supplementary data.

0040-4039/$ - see front matter © 2012 Elsevier Ltd. All rights reserved.
http://dx.doi.org/10.1016/j.tetlet.2012.09.036

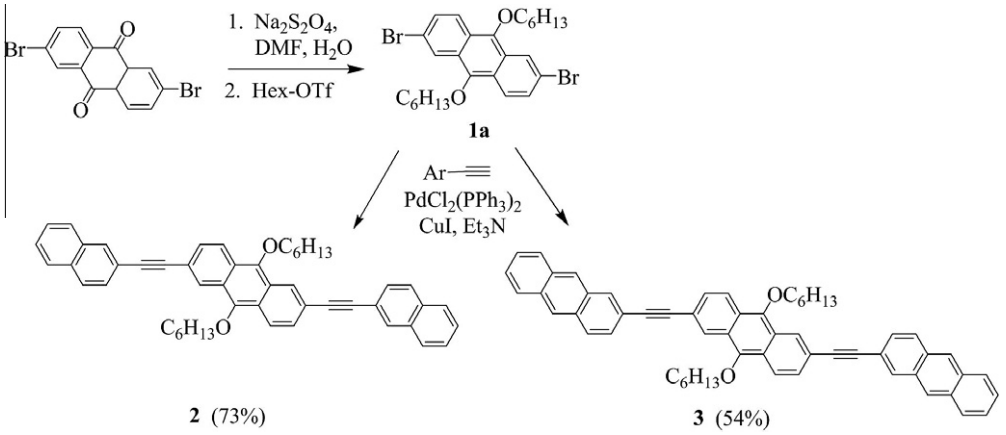

Scheme 1. Synthesis of compounds **2** and **3**.

1,2-dichloroethane and *n*-hexane to give large, prismatic crystals. In light of these encouraging results, a series of these compounds (**4b–4e**) were similarly prepared in order to determine what effects chain length and branching of the alkyl substituent play in the solubility and morphology of these compounds.

Each of the compounds **4a–4e** was crystallized to give orange–red solids. However, the compounds showed remarkable differences in crystal formation. While hexyl and 2-ethylhexyl analogs **4a** and **4d** gave fairly large, prismatic crystals, it was found that either longer or shorter alkyl chains resulted in small, needlelike crystals (Fig. 1). The isobutyl derivative (**4b**) gave intermediate results, producing thicker needles which were sufficient for X-ray analysis.[§]

X-ray analysis showed that crystals of both compounds **4a** and **4b** are monoclinic, space group number 14 ($P2_1/c$ and $P2_1/n$ respectively) and pack with herringbone, edge-to-face type arrangements (Fig. 2). Under the crystallization conditions employed, compound **4b** stacked into tight 1-dimensional slip-stacks having an offset of 3.356(2)Å. Compound **4a**, with its larger solubilizing chain, incorporated *n*-hexane as occluded solvent. The X-ray data for compound **4a** show that this compound has a greater distance between molecules within each columnar stack, with the space occupied by the hexyl chains between the peripheral acene moieties and occluded *n*-hexane solvent between the central acene. On the other hand, the individual columns in **4a** interdigitate more effectively. A comparison of the overlap of individual slip-stacks may be seen by comparison of the images viewed from the b axis (Fig. 2, right hand side).

Each of the compounds prepared was yellow in solution and strongly fluorescent. Compounds **2** and **3**, in which the exterior rings were coupled at the 2-positions, showed a much stronger absorbance in the 300–350 nm range, with weaker bands extending out to 450–460 nm. In contrast, compounds **4a–e** exhibited five strong bands stretching to wavelengths slightly greater than 500 nm (Fig. 3a, Table 1).[¶] It was found that the intensities of the different bands and the onset of absorption showed subtle differences as a function of concentration and solvent, suggesting aggregation effects may contribute to the longer wavelength bands.[‖]

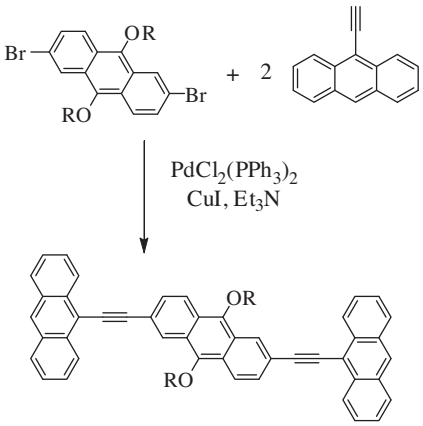

Scheme 2. Synthesis of compound set **4**.

Photoluminescence spectroscopy of **4a** showed fluorescence in the 480–620 nm range, with a maximum at 505 nm (Fig. 3b).

Absorbance spectra for series **4** were also measured on thin films. The absorption onsets of the thin films were red-shifted relative to the solution spectra by 30–40 nm, indicating that, as expected, some degree of intermolecular pi-overlap was occurring in the thin films (Fig. 4). For both solution and thin-films, the spectra for these compounds were very similar. Although we had postulated that the different alkyl substituents might cause conformational changes which would affect the electronics of the pi system, the spectral data present no evidence that this has occurred.

Next, the oxidative potentials of these compounds were measured by cyclic and differential-pulse voltammetry. In the range studied, compounds in series **4** exhibited two quasi-reversible oxidations at approximately +0.57 and +0.76 V relative to a Ferrocene/Ferrocenium reference (Fig. 5). Coupling these findings with the absorbance onsets (510 nm for each compound in set **4**, varying slightly with concentration), the solution-phase HOMO–LUMO energies of these compounds in solution were estimated to be around −5.37 and −2.93 eV, respectively (Table 1). These values are comparable to HOMO–LUMO energies reported the anthracenes bearing 9,10-arylethynyl derivatives.[8]

[§] CCDC 894995 and 894996 contain the supplementary crystallographic data for this Letter. These data can be obtained free of charge from The Cambridge Crystallographic Data Centre via www.ccdc.cam.ac.uk/data request/cif.

[¶] Molar absorptivities for each compound at multiple wavelengths are tabulated in the Supplementary data.

[‖] Absorbance spectra in toluene and dichloromethane at various concentrations are provided in the Supplementary data

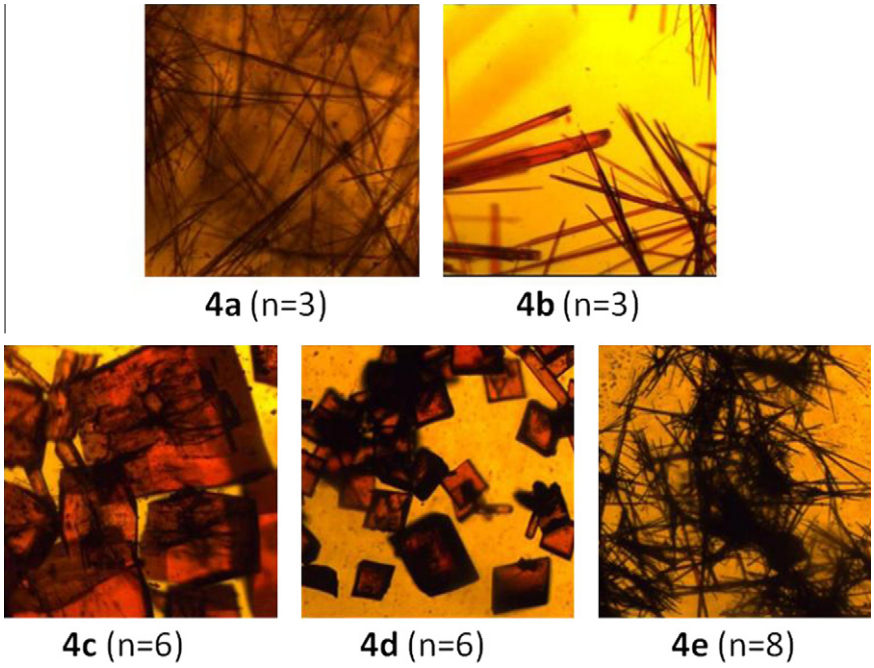

Figure 1. Crystal morphology versus chain length for compound series 4. *n* = number of carbons in parent alkyl chain. Images shown are 1 mm on each side.

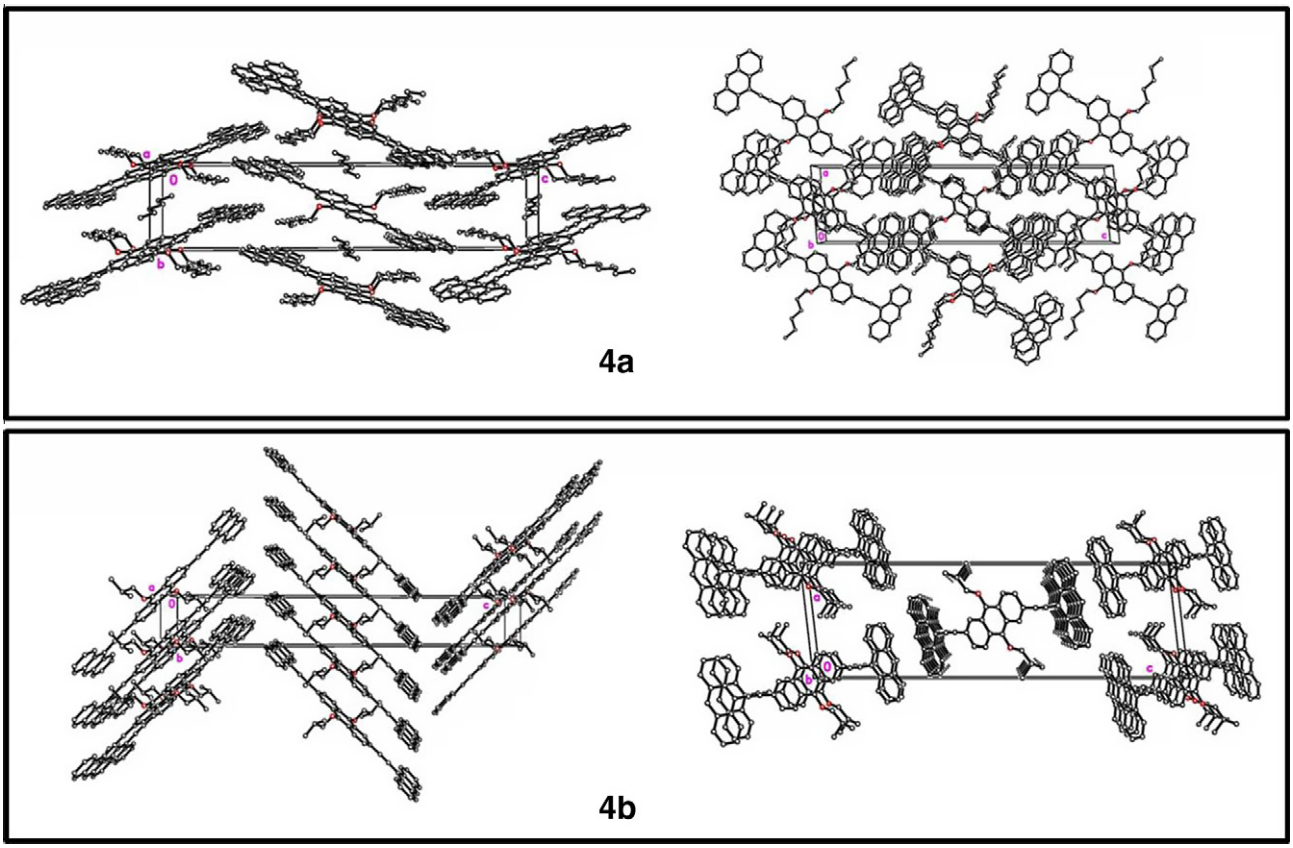

Figure 2. X-ray crystallographic images showing the crystal packing for compounds **4a** (top) and **4b** (bottom), viewed from crystallographic a (left) and b (right) axes.

It was found that compounds in series **4** were susceptible to gradual degradation when stored at room temperature. The most pronounced degradation was observed for the octyl derivative **4e**, and it is possible that this degradation correlates with the lower yields obtained in the synthesis of this compound as compared with others in the series. The lack of stability suggests that further functionalization of these compounds (likely with electron-withdrawing substituents on the outer ring) will be

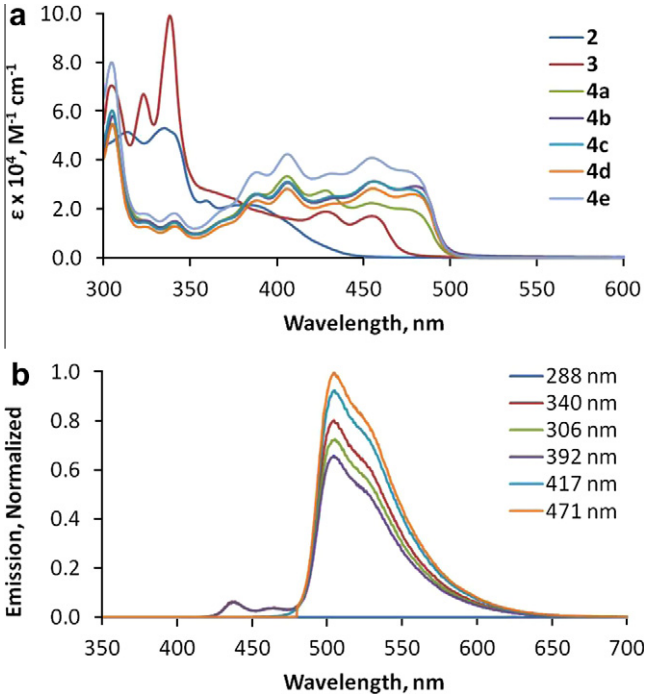

Figure 3. (a) Solution-phase UV–Vis spectra for compounds **2–4** (each compound 10 μM in toluene); (b) PL spectra of compound **4a**, using λ_{ex} of 288–471 nm.

Table 1
Measured absorption and HOMO–LUMO energies

	λ_{max} (nm)	λ_g^{opt} (eV)[a]	ΔE_{ox} (eV)	HOMO (eV)[b,c]	LUMO (eV)[d]
4a	304, 405, 455, 479	2.43	+0.58	−5.38	−2.95
4b	304, 404, 456, 484	2.43	+0.56	−5.36	−2.93
4c	304, 404, 455, 477	2.43	+0.57	−5.37	−2.94
4d	405, 400, 458, 484	2.43	+0.56	—[e]	—
4e	305, 408, 454, 481	2.43	+0.56	—	—

[a] Calculated based on absorbance onset in solution UV.
[b] Voltage relative to Ferrocene standard.
[c] Calculated using Eox (Ferrocene) = 4.8 eV.
[d] HOMO (eV)−E_g^{opt} (eV).
[e] Not measured.

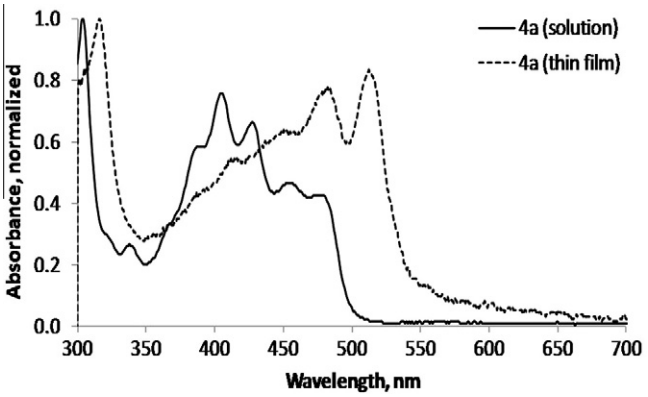

Figure 4. Comparison of solution and thin-film spectra for compound **4a**.

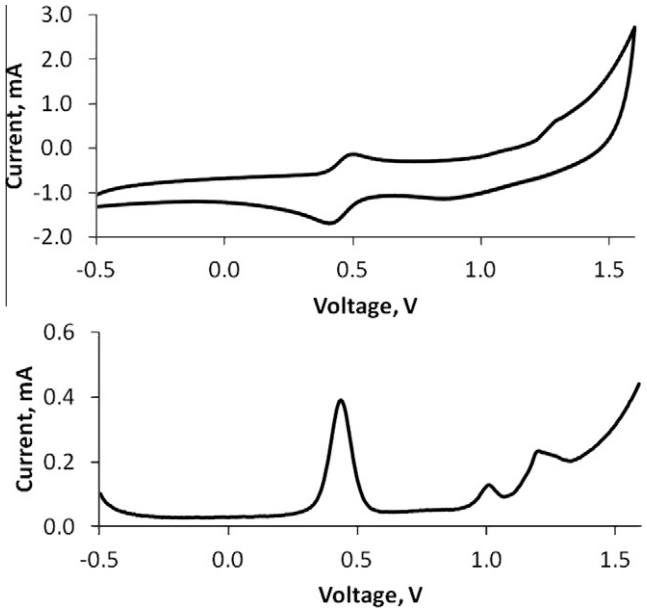

Figure 5. CV and DPV Curves for compound **4a**.

necessary before compounds in this platform are viable for material applications.

A number of conclusions may be drawn from these initial results. First, the enhanced solubility and longer-wavelength absorptions clearly indicate that the 9′-anthracyl species (**4a–e**) have greater potential than the 2′-naphthyl (**2**) and 2′-anthracyl (**3**) with regard to thin-film semiconducting applications. Second, it was found that the alkoxy substituent contributes significantly to the solubility and crystal packing of series **4**, with the hexyl- and 2-ethylhexyl- analogs (**4a** and **4d**) crystallizing most readily. Surprisingly, lengthening the alkyl chain beyond six carbons did not appear to enhance crystallinity, and lower yields, more difficult purification, and an increased rate of decomposition was qualitatively observed with the octyl substituent. Among series **4**, each compound evaluated exhibited a HOMO–LUMO energy gap of ~2.4 eV, consistent with values reported previously for 9,10-bis(arylethynyl)anthracenes. X-ray analysis showed that the compounds pack into a herringbone arrangement. While this packing motif should correlate well with application in organic photovoltaic devices, further functionalization around the 2,6-diarylethynylanthracene platform will be necessary to optimize the stability, electronic parameters, and morphology of these compounds for this application.

Although the oxygens of the 9,10-bis(hydroxyl)anthracene system provide a convenient handle for functionalization, the electron-donating alkoxy groups activate the electron-rich acene system to oxidation and/or electrophilic substitution, and it is likely that the gradual decomposition observed for these compounds is correlated to this enhanced electron density. In light of this, additional compounds are being explored in which the alkoxy substituents are replaced with much less electron-donating substituents, and compounds in which the alkoxy substituents on the center ring are complimented by electron-withdrawing groups on the periphery.

Acknowledgments

This material is based upon work supported by the Kentucky NASA EPSCoR program, by the National Science Foundation under CHE-0922033, by the Jones/Ross Research Center at Murray State University, and by the Murray State University Committee on Institutional Research. X-ray data were collected using both a Nonius KappaCCD diffractometer and a Bruker Nonius X8 Proteum diffractometer obtained with funding from the NSF (MRI grant No.

0319176). The authors also wish to thank Daniel Johnson (Murray State University) for his assistance with the electrochemical and photoluminescence analyses.

Supplementary data

Supplementary data associated with this article can be found, in the online version, at http://dx.doi.org/10.1016/j.tetlet.2012.09.036. These data include MOL files and InChiKeys of the most important compounds described in this article.

References and notes

1. Marks, T. J. *MRS Bull.* **2010**, *35*, 1018.
2. Yamashita, Y. *Sci. Technol. Adv. Mater.* **2009**, *10*, 024313.
3. Anthony, J. E. *Angew. Chem., Int. Ed.* **2008**, *47*, 452.
4. Silvestri, F.; Marrocchi, A. *Int. J. Mol. Sci.* **2011**, *11*, 1471.
5. Murphy, A. R.; Frechet, J. M. J. *Chem. Rev.* **2007**, *107*, 1066.
6. Facchetti, A. *Mater. Today* **2007**, *10*, 29.
7. Anthony, J. E. *Chem. Rev.* **2006**, *106*, 5028.
8. Silvestri, F.; Marrocchi, A.; Seri, M.; Kim, C.; Marks, T. J.; Facchetti, A.; Taticchi, A. *J. Am. Chem. Soc.* **2010**, *132*, 6108.
9. Jung, K. H.; Bae, S. Y.; Kim, K. H.; Cho, M. J.; Lee, K.; Kim, Z. H.; Choi, D. H.; Lee, D. H.; Chung, D. S.; Park, C. E. *Chem. Commun.* **2009**, 5290.
10. Bae, S. Y.; Jung, K. H.; Hoang, M. H.; Kim, K. H.; Lee, T. W.; Cho, M. J.; Jin, J.-I.; Lee, D. H.; Chung, D. S.; Park, C. E.; Choi, D. H. *Synth. Met.* **2010**, *160*, 1022.
11. Zhang, C. H.; Guo, E. Q.; Zhang, Y. L.; Ren, P. H.; Yang, W. J. *Chem. Mater.* **2009**, *21*, 5125.
12. Abou-Elkhair, R. A. I.; Dixon, D. W.; Netzel, T. L. *J. Org. Chem.* **2009**, *74*, 4712.